Optimization, thermodynamic and economic analysis of a regenerative ORC for WHR in manufacturing process of cement

Felipe Arrieta and Luiz Fernando Moreira

August 10, 2018

Optimization, thermodynamic and economic analysis of a regenerative ORC for WHR in manufacturing process of cement

***Felipe R. P. Arrieta*[a, b], *Luiz F. Moreira*[a]**

[a] *Pontifical Catholic University of Minas Gerais, Belo Horizonte, Brazil, felipe.ponce@pucminas.br*
[b] *Ibmec, Belo Horizonte, Brazil*

Abstract:

This paper aims to investigate the thermodynamic effectiveness of a regenerative organic Rankine cycle (ORC) working under subcritical and subcritical with superheating operating conditions for waste heat recovery (WHR) in order to produce electric energy from exhaust gases originated in cement production process. In addition, a methodology for working fluid selection based on fluids' safety and environmental aspects, thermodynamic characteristics and slope of saturated vapour curves was employed. Also, an economical assessment of the cycle applying the organic fluids with higher thermodynamic results was carried out. The system was designed and optimized using the Genetic Algorithm (GA) method in the Engineering Equation Solver (EES) software. According to the results, the subcritical with superheating ORC was more efficient compared to the subcritical one in terms of net power output generated (2.06%), thermal (3.10%) and exergy (2.99%) efficiencies. Moreover, the isentropic fluid R141b demonstrated the highest performance in the subcritical condition. Whereas another isentropic fluid, R11, reached the best effectiveness in the subcritical with superheating scenario. From the economical point of view, the specific investment and specific electricity generation costs of the subcritical condition with superheating were lower than those of the subcritical one, with amounts of 3.46% and 1.31%, respectively.

Keywords:

Cement industry, Genetic algorithm, Organic Rankine cycle, Waste heat recovery.

1. Introduction

As stated by [1], the costs of electric energy consist of, approximately, 25% of all operational expenses in cement industry. Additionally, waste heat recovery (WHR) technologies, such as cogeneration systems through organic Rankine cycles (ORC), are capable of providing up to 30% of the whole electricity needs of a cement factory. Due to the organic fluids' aspects, the ORC provides interesting advantages over the conventional Rankine cycle (RC) when operating with temperatures from 80 to 400°C as: good effectiveness, wide commercial availability, competitive operational and maintenance costs, simple construction, great adaptability to different heat sources, etc [2-6]. Another important benefit of the ORC mentioned by [7] is that isentropic and dry organic fluids do not demand superheating before entering the turbine inlet as water does and this prevents risk of erosion on the turbine blades. Furthermore, it is possible to classify the ORC working fluids in accordance with their safety and environmental characteristics as stated by [8]. Moreover, the organic working fluids can be evaluated considering their saturation vapor curves in (i) dry, with positive slopes after the critical point; (ii) wet, with negative slopes after the critical point; and (iii) isentropic, with approximately a vertical saturation vapor curve [9].

As suggested by [10], the ORC overall performance can be improved by including other equipment to the cycle, for example, regenerators, reheaters, extraction steam turbines, etc. Nonetheless, this might influence the system's installation and operational costs. As argued by [11], the costs of a cogeneration system deserve to be highlighted due to their significant importance for the project's viability. Also, the costs involved in an ORC are completely associated with the net power output generated by the cycle and its heat source temperature.

This paper aims to study the thermodynamic efficiency of a regenerative ORC working under subcritical and subcritical with superheating operating conditions in a typical Brazilian cement plant with a clinker productive capacity of 3,500 ton/day.

2. Methodology

The procedures for working fluid selection are described below as well as the cogeneration system specification, its thermodynamic and economical modeling.

2.1. Working fluid selection

Firstly, 42 pure refrigerant fluids acquired from [8] were investigated and their availability was verified in EES database, since it was the software supplied by the institution to develop this study. Then, 17 working fluids were discarded as a result of their thermodynamic properties not being available in the software database. From the safety point of view, all organic fluids were considered eligible for this study, by reason of their null or acceptable flammability and toxicity levels. Beyond this, these fluids do not present risk of explosion due to their high dispersal speed into the air as emphasized by [12]. From the environmental perspective, 7 working fluids were eliminated by virtue of their atmospheric lifetime being higher than 100 years. In a further step, the organic fluids were assessed according to their quality at the turbine outlet in an ideal ORC and their thermodynamic properties, for instance, critical temperature (T_{cr}), critical pressure (P_{cr}) and saturation pressure at the condenser outlet ($P_{sat\ cond}$). Based on these criteria, 10 more working fluids were removed and the selected organic fluids for this study are shown in Table 1. The working fluid selection performed in this work applied the methodology proposed by [13] in their study.

After selecting the most suitable organic fluids for this study, the operating parameters of the ideal ORC were examined. In order to coordinate the results of the optimization performed afterwards with the working fluid selection in this section, during the simulation of the ideal ORC, the pressure at the turbine inlet that led the cycle to experience its greatest efficiency from the context of specific net power output was identified for each working fluid. Thus, this pressure, named as optimum operating pressure ($P_{1,opt}$), was utilized as an inlet data in the designed system.

Table 1. Organic working fluids selected for application in this work

Fluid	Safety group	ODP	GWP_{100}	Atmospheric lifetime (years)	T_{cr} (°C)	P_{cr} (MPa)	$P_{sat\ cond}$ (MPa)	Quality at the turbine outlet min - max (-)	Classification
R11	A1	1.00	4,750	45	198.00	4.41	0.130	0.852 - 0.989	Isentropic
R124	A1	0.022	609	5.8	122.28	3.62	0.470	0.959 - 1.000	
R141b	-	0.11	725	9.3	204.20	4.25	0.101	0.962 - 1.000	
R142b	A2	0.065	2,310	17.9	137.11	4.06	0.420	0.929 - 0.999	
R600	A3	0.00	~20	0.018	151.98	3.80	0.300	0.951 - 1.000	
R600a	A3	0.00	~20	0.019	134.67	3.64	0.430	0.926 - 1.000	
R123	B1	0.02	77	1.3	183.68	3.67	0.120	0.984 - 1.000	Dry
R245fa	B1	0.00	1,030	7.6	154.01	3.65	0.190	0.977 - 1.000	

2.2. System characterization

Thermal energy from the suspension preheater exhaust gas and hot air derived from the clinker cooler discharge were used simultaneously to produce electric energy. Instead of using a simple ORC arrangement, which is a commonplace topic in the investigated literature, a regenerative ORC configuration was proposed based on the arguments presented by [10] and [14] aiming to achieve the highest performance as possible for an ORC. As explained by [10] and [14], the regenerative ORC overall effectiveness is greater than the simple one due to its higher thermodynamic mean temperature during the heat addition process and lower irreversibilities within the cycle provided by additional equipment as regenerator, direct contact heater, multi-stage turbine with steam extractions, etc.

Therefore, the proposed regenerative ORC was comprised of a three stage turbine (TURB) with two steam extractions, condenser (COND), centrifugal pumps (PP 01 and PP 02), direct contact heater (DCH), regenerator (REG), liquid drain trap (TRAP) and an evaporation unit, which was composed of economizer (ECO), two evaporators (EVP 01 and EVP 02) and a superheater (SPH). Further components used were: electric generator (GEN), electrical substation (SEE) and electric motor (M). The regenerative ORC for WHR in cement production process analyzed in this study is illustrated in Fig. 1. The working principle of the conceived ORC can be described as: heat is provided to the organic fluid at constant pressure in the evaporation unit (process 9-1); the working fluid is expanded in the turbine (process 1-4). However, before finishing the expansion, it experiences two steam extractions (processes 1-2 and 1-3). These steam extractions are sent to the direct contact heater and to the regenerator, correspondingly. After accomplishing the expansion process in the turbine, the working fluid transfers heat to the cooling water at constant pressure in the condenser (process 4-5) and it is pumped to the regenerator (process 5-6), where it receives heat from the second steam extraction (process 3-16) at constant pressure as well. After going through the regenerator (process 6-7), the organic fluid is mixed with the first steam extraction coming from the turbine and, in the meantime, the condensed organic fluid (process 16-17) is sent back to the condenser. Lastly, the working fluid leaves the direct contact heater and it is pumped back to the evaporation unit (process 8-9) to restart the cycle.

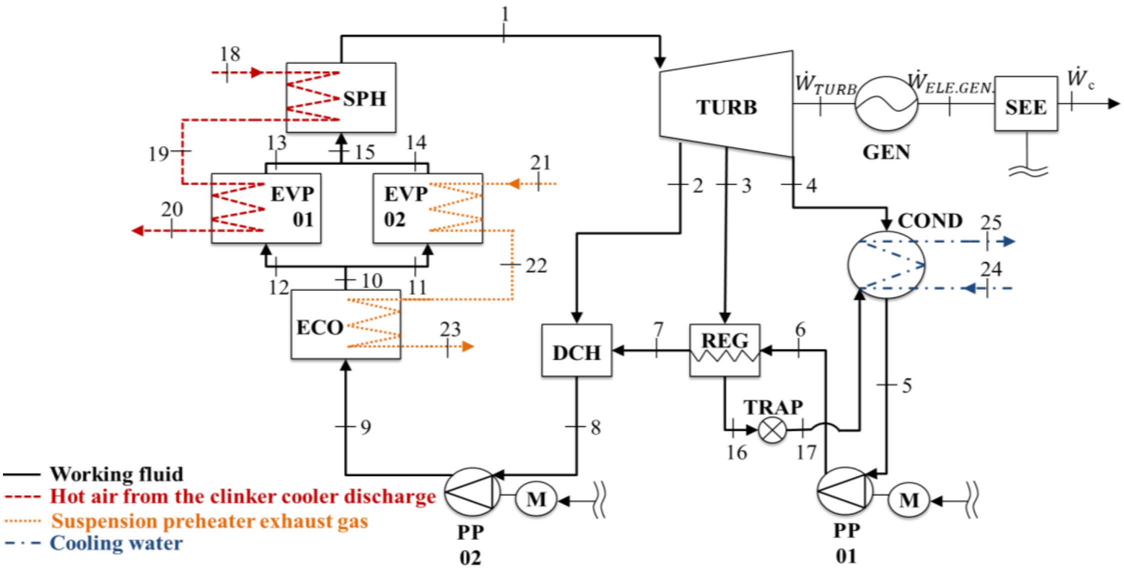

Fig. 1. Regenerative ORC for WHR in cement industry.

2.3. Thermodynamic modeling

In agreement with the first and second laws of thermodynamics, the principal operational parameters of the modeled ORC were calculated as follows:

The total amount of heat received by the organic fluid in the evaporation unit is given by (1):

$$\dot{Q}_{EVP\ UN} = \dot{m}(h_1 - h_9), \qquad (1)$$

where h_1 and h_9 are the specific enthalpies of the working fluid at the evaporation unit outlet and inlet, subsequently, and $\dot{m}$ is the mass flow rate of organic fluid.

The power generated by the three stage turbine can be expressed as (2):

$$\dot{W}_{TURB} = \dot{m}h_1 - (\dot{m}_2h_2 + \dot{m}_3h_3 + \dot{m}_4h_4), \qquad (2)$$

where h_2, h_3 and h_4 are the specific enthalpies of the fraction of organic fluid at each stage of the turbine outlet, and $\dot{m}_2$, $\dot{m}_3$ and $\dot{m}_4$ are the portions of the total mass flow rate at each stage of the turbine outlet as well.

The power consumed by the pumps 01 and 02 are determined by (3) and (4), in this order:

$$\dot{W}_{PP\ 01} = \dot{m}_4(h_6 - h_5), \qquad (3)$$

$$\dot{W}_{PP\,02} = \dot{m}(h_9 - h_8), \quad (4)$$

where h_6 and h_5 are the specific enthalpies of the working fluid at the pump 01 outlet and inlet, respectively, and h_9 and h_8 are the specific enthalpies of the organic fluid at the pump 02 outlet and inlet, correspondingly.

The net power output produced by the system is indicated in (5):

$$\dot{W}_c = \eta_{GEN}\dot{W}_{TURB} - \left(\dot{W}_{PP\,01} + \dot{W}_{PP\,02}\right), \quad (5)$$

where η_{GEN} is the efficiency of the electric generator.

The first law efficiency of the cycle is given by (6):

$$\eta_{th} = \frac{\dot{W}_c}{\dot{Q}_{EVP\,UN}}, \quad (6)$$

The physical exergy of each thermodynamic state can be expressed as (7):

$$ex = h - h_0 - T_0(s - s_0), \quad (7)$$

where h is the specific enthalpy of the stream, h_0 is the specific enthalpy of the stream assessed in the pressure and temperature of the dead state, T_0 is the temperature of the dead state (see Table 4), s is the specific entropy of the stream and s_0 is the specific entropy of the stream evaluated in the pressure and temperature of the dead state.

The exergy destruction within the control volume by action of irreversibilities is determined by (8):

$$\dot{E}_{gen} = T_0\dot{\sigma}_{cv}, \quad (8)$$

where $\dot{\sigma}_{cv}$ is the entropy generation inside the control volume.

The second law efficiency of the ORC is indicated in (9):

$$\eta_{ex} = \frac{\dot{P}}{\dot{F}}, \quad (9)$$

where $\dot{P}$ is the exergy product; and $\dot{F}$ is the exergy fuel.

Additionally, the condenser was established as a shell-tube heat exchanger and the other heat exchangers were designed as a crossflow one fluid unmixed configuration. Furthermore, the surface area of heat transfer was calculated employing the logarithmic mean temperature difference (LMTD) method as given in (10):

$$\dot{Q}_i = U_i A_i F_i \Delta T_i^{LMTD}, \quad (10)$$

where the subscript "i" refers to the analyzed heat exchanger, $\dot{Q}$ is the heat transfer rate obtained from the energy rate balance equation, U is the overall heat transfer coefficient provided by [15] as demonstrated in Table 2, A is the surface area for heat transfer, F is a dimensionless correction factor related to the heat exchanger configuration and its inlet and outlet temperatures, which is calculated using an internal function in the EES software, and ΔT_i^{LMTD} is the logarithmic mean temperature difference expressed as (11).

Table 2. Overall heat transfer coefficients for type of interaction

Equipment	Type of interaction	U (W/m²-K)
Condenser	Liquid/Gas-Liquid	350.00
Regenerator	Liquid/Gas-Liquid	400.00
Economizer and Evaporators 01/02	Liquid-Gas	80.00
Superheater	Gas-Gas	90.00

$$\Delta T_i^{LMTD} = \left[\frac{(T_{h,out} - T_{c,in}) - (T_{h,in} - T_{c,out})}{ln\left(\frac{T_{h,out} - T_{c,in}}{T_{h,in} - T_{c,out}}\right)} \right], \quad (11)$$

where $T_{h,out}$ is the hot stream temperature at the heat exchanger outlet; $T_{c,in}$ is the cold stream temperature at the heat exchanger inlet; $T_{h,in}$ is the hot stream temperature at the heat exchanger inlet; and $T_{c,out}$ is the cold stream temperature at the heat exchanger outlet.

The system operated under subcritical and subcritical with superheating conditions. The chemical composition of the exhaust gases from cement production process as well as their outlet temperature from the evaporation unit were acquired from [16] and are compiled in Table 3. This is a real cement factory able to produce 3,500 tons of clinker per day and it is located in Quixeré, CE, Brazil.

Table 3. Exhaust gases from cement production process inlet data

Hot air from the clinker cooler discharge data:				Suspension preheater exhaust gas data:			
Variable		Unit	Value	Variable		Unit	Value
Molar composition:	N_2	%	79.00	Molar composition:	CO_2	%	26.30
	O_2	%	21.00		N_2	%	64.58
					O_2	%	4.94
					H_2O	%	4.18
Inlet / Outlet temperature		ºC	440.00 / 114.00	Inlet / Outlet temperature		ºC	310.00 / 228.00
Mass flow rate		kg/s	48.15	Mass flow rate		kg/s	88.03

In addition, the isentropic efficiencies of the pumps and turbine were obtained from [17] and the most relevant assumptions for simulating cogeneration systems are summarized in Table 4. This information is widely adopted in the studied literature.

Table 4. Additional inlet data considered in the thermodynamic modeling

Variable	Unit	Value
Isentropic efficiency of the pumps / turbine	%	70.00 / 85.00
Efficiency of the electric generator / motor	%	98.50 / 99.00
Pressure of the exhaust gases from cement production process	MPa	0.101
Environment pressure (P_0) / temperature (T_0)	MPa / °C	0.101 / 22.00

The cycle was also developed considering that: (i) it worked at a steady state; (ii) the variations of kinetic and potential energies were neglected; and (iii) all processes were adiabatic. The simulations were performed using the EES Professional V.10.092 software.

2.4. Economical modeling

The method for cost estimating established for this study was proposed by [15] and it takes into account the main operational parameters of each type of equipment, such as power produced by the turbine, surface area for heat transfer of the heat exchangers, power consumed by the pumps, etc. The construction material assumed for all components was stainless steel as recommended by [18].

The specific investment cost, which is the ratio between the total capital cost and the net power output generated by the system, was calculated applying the equation indicated in (12):

$$I = \frac{I_T}{\dot{W}_c}, \quad (12)$$

where I_T is the system total capital cost determined by (13). It includes costs with installation, operation and maintenance required by the equipment in the ORC.

$$I_T = \sum_i C_{BM,i} \frac{IF_{2004}}{IF_{2016}} (C_C + C_F)(C_{SD} + C_{AB} + C_{OS}), \qquad (13)$$

where the subscript "i" refers to the components of the cycle, $C_{BM,i}$ are the direct and indirect expenses with an equipment, for instance, its purchase price, materials for installation, direct labor, freight, insurance, taxes and contractor engineering expenditures, IF_{2004} and IF_{2016} are the dimensionless index factors for the years of 2004 and 2016 acquired from [19], which correspond to 124 and 100, subsequently, C_C and C_F are the costs with contingency and fees, in this order, and their sum is equivalent to 1.18, and C_{SD}, C_{AB} and C_{OS} are the expenses with the site development, auxiliary buildings and off-site facilities, respectively, which their sum is equals to 1.30.

Finally, the specific electricity generation cost can be calculated by (14):

$$C = I \frac{AF}{OH} + C_{O\&M}, \qquad (14)$$

where AF is the amortization factor expressed as (15), OH is the amount of operating hours per year and it was considered to be 8,030 hours/year, and $C_{O\&M}$ is the specific cost of operation and maintenance, which is equivalent to 0.02 $/kWh in accordance with [20].

$$AF = \frac{j(1+j)^n}{(1+j)^n - 1}, \qquad (15)$$

where j is the annual interesting rate of 7.00% and n is the system lifecycle equals to 20 years.

The cost estimating was performed in American dollars (USD-$) converted to Brazilian currency (BRL-R$) with an exchange rate of 3.2585 R$/$. Furthermore, the exhaust gases from cement industry, which would be released into the atmosphere, were assumed to be available at cost-free.

2.5. Optimization

Initially, the optimization of the cycle's operating parameters under subcritical and subcritical with superheating conditions in this study had the objective of finding the largest amount of net power output produced by each working fluid selected earlier. Hence, the net power output, adopted as the principal operational parameter in this study, was defined as the objective function. Other operational parameters were also optimized with the purpose of verifying their influence on one another's results. For this reason, the maximization of exergy efficiency and minimization of specific investment and specific electricity generation costs were determined as objective functions afterwards.

The temperature difference at the economizer ($\Delta T_{sub\text{-}cooling}$) and evaporator 02 ($\Delta T_{EVP\ 02}$) were optimized in both operating conditions. Whereas, the temperature variation at the turbine inlet ($T_{TURB\ in}$) and evaporator 01 ($\Delta T_{EVP\ 01}$) were optimized only in subcritical with superheating condition. The range of variation for the variables considered in the optimization procedure and the pressure ratio at the turbine stages are given in Table 5.

Table 5. Range of variation of the operating parameters during the optimization

Fluid	P_2/P_1	P_3/P_1	$\Delta T_{sub\text{-}cooling}$ min - max (°C)	$\Delta T_{EVP\ 01}$ min - max (°C)	$\Delta T_{EVP\ 02}$ min - max (°C)	$\Delta T_{TURB\ in}$ min - max (°C)
R11	0.25	0.10	31 - 66	100 - 200	100 - 200	T_1 at $P_{1,opt}$ - 400°C
R123	0.25	0.15	44 - 67			
R124	0.20	0.15	41 - 61			
R141b	0.25	0.10	45 - 67			
R142b	0.20	0.15	36 - 66			
R245fa	0.20	0.10	52 - 66			
R600	0.20	0.15	62 - 71			
R600a	0.20	0.15	49 - 65			

3. Results and discussion

The optimization results and economical assessment are exhibited and discussed in this section.

3.1. Thermodynamic results with optimization of $\dot{W}_c$

Firstly, the optimization of the subcritical condition was accomplished and the most important results achieved as heat supplied to the system, mass flow rate at the turbine inlet, net power output, exergy destruction, thermal and exergy efficiencies are compiled in Table 6. According to the obtained results, it was possible to identify that the isentropic fluids R141b, R11 and the dry fluid R123, in this order, demonstrated to be more advantageous than the other organic working fluids in terms of net power output, first and second laws efficiencies.

Table 6. Results of the regenerative ORC working under subcritical condition

Fluid	Classification	$\dot{Q}_{EVP\ UN}$ (kW)	$\dot{m}$ (kg/s)	$\dot{W}_c$ (kW)	η_{th} (%)	η_{ex} (%)	$\dot{E}_d$ (kW)
R11	Isentropic	24,255	158.65	5,535	21.72	48.22	5,658
R124		24,259	171.99	3,186	13.10	29.08	7,750
R141b		24,168	118.08	5,541	22.40	49.70	5,478
R142b		24,259	127.49	3,703	15.03	33.35	7,283
R600		24,258	63.33	4,001	16.32	36.23	6,969
R600a		24,253	69.18	3,434	14.01	31.09	7,529
R123	Dry	24,257	151.28	4,964	20.46	45.41	5,964
R245fa		24,261	127.90	4,090	16.82	37.34	6,848

Moreover, with the purpose of illustrating the net power output increment during the optimizations, Fig. 2 exhibits the net power output produced by the ORC without optimization and the net power output increase after the optimization in the T-s diagram for the three organic fluids with higher performance. It was observed that the optimization presented a slight, but valuable, improvement in the cycle's thermodynamic results from the perspective of net power output generated.

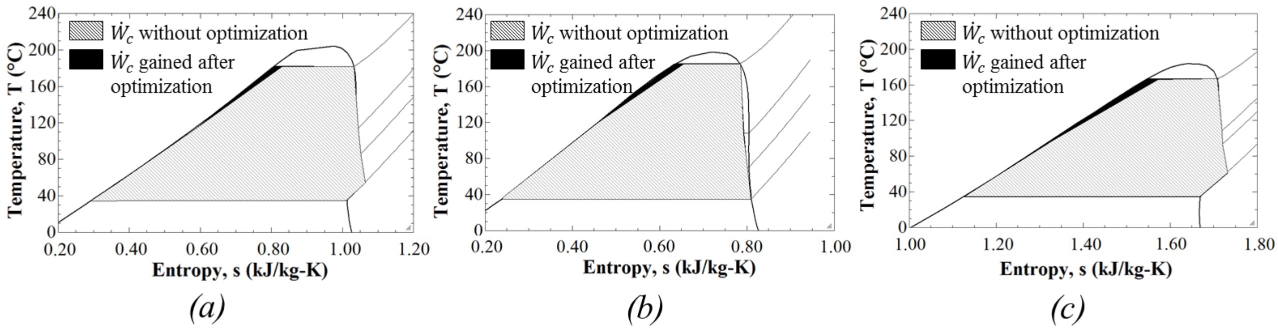

Fig. 2. T-s diagrams of the subcritical ORC: a) R141b, b) R11 and c) R123.

Similarly to the subcritical condition, an analogous method was carried out for simulating and optimizing the cycle working under subcritical with superheating condition. The acquired results in this step, for example, heat required by the ORC, mass flow rate at the turbine inlet, net power output, exergy destruction, thermal and exergy efficiencies are summarized in Table 7. Contrary to what was observed in the results of the subcritical ORC, in this operating condition the isentropic fluid R11 performed better from the point of view of net power output, first and second laws efficiencies followed by the other isentropic fluid, R141b, and the dry fluid R123, correspondingly. This result can be justified by the decrement in entropy generation within the system components provided by the subcritical with superheating operating condition. In addition, the fluid R11 reached the most substantial reduction in exergy destruction (7.09%) in contrast with R141b (2.41%) and R123 (0.17%).

Table 7. Results of the regenerative ORC working under subcritical with superheating condition

Fluid	Classification	$\dot{Q}_{EVP\,UN}$ (kW)	$\dot{m}$ (kg/s)	$\dot{W}_c$ (kW)	η_{th} (%)	η_{ex} (%)	$\dot{E}_d$ (kW)
R11	Isentropic	23,676	112.10	5,614	22.85	50.59	5,284
R124		23,842	122.36	3,289	13.65	30.13	7,545
R141b		24,177	90.34	5,547	22.49	50.19	5,349
R142b		24,097	84.78	3,902	16.01	35.52	7,004
R600		24,076	42.59	3,882	16.12	35.72	6,983
R600a		24,231	39.70	3,290	13.44	29.81	7,667
R123	Dry	24,253	108.56	4,975	20.51	45.52	5,954
R245fa		23,930	97.06	4,191	17.31	38.28	6,681

As illustrated for the net power output enhancement during the optimization of the subcritical ORC, Fig. 3 demonstrates the acquired gain in terms of net power output produced by the subcritical with superheating ORC for the three working fluids with greater results. It was possible to verify that there was a modest increment in the amount of net power output when optimizing this configuration as well.

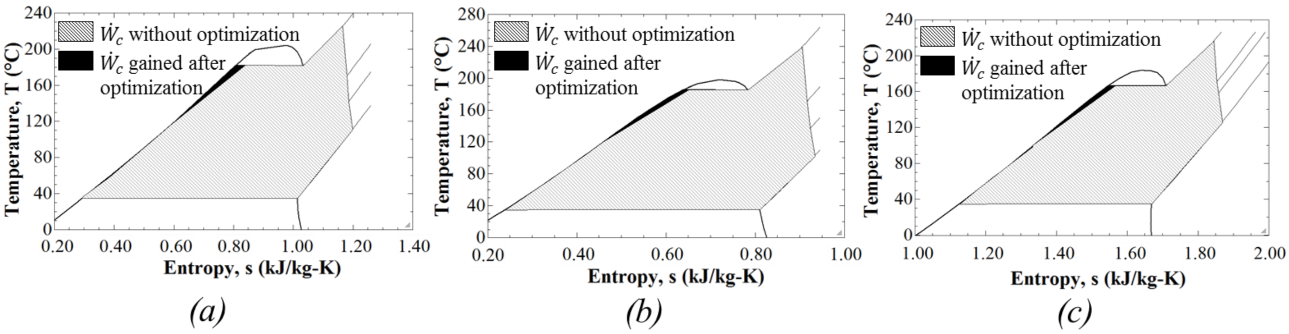

Fig. 3. T-s diagrams of the subcritical with superheating ORC: a) R141b, b) R11 and c) R123.

A detailed comparison among the acquired results revealed that the cycle achieved the highest amounts of net power output, thermal and exergy efficiencies when operating under the subcritical with superheating condition for most of the investigated organic fluids. The exceptions were the isentropic fluids R600 and R600a, which presented inferior results in this operating condition contrasted to the subcritical one. This fact is explained by the growth in entropy generation within the ORC equipment supplied by these two fluids, which led to a rise in terms of irreversibilities and losses and, consequently, a decline in the system performance. As a result, it indicates that these fluids are inadequate to work in the studied circumstances. On the other hand, when this setback was neglected, the increment in the results of the cycle with the other six working fluids from the perspective of net power output, first and second laws efficiencies corresponded to, in averages of, 2.06%, 3.10% and 2.99%, subsequently. These results are shown in Fig. 4, which illustrates the relation between the subcritical and subcritical with superheating operating conditions results for the net power output (Fig. 4a) and thermal efficiency (Fig. 4b) with the chosen organic fluids.

The effectiveness gain in the subcritical with superheating condition compared to the subcritical one was predictable by reason of the organic working fluid temperature enhancement at the turbine inlet as a consequence of the increase in the thermodynamic average temperature during the heat addition process in the evaporation unit provided by the superheater. Another benefit of improving the average temperature while adding heat to the cycle was the less amount of thermal energy required by the subcritical with superheating condition from the heat source for evaporating the organic fluid in contrast with the subcritical ORC. This enabled the system when operating under subcritical with superheating condition to work more efficiently from the context of first law efficiency. An additional factor to be pointed out is that the entropy production decreased in most components of the cycle working under the subcritical with superheating operating condition. It is justified by the decrement in exergy destruction within the ORC equipment, which was the reason for the rise in the system second law efficiency.

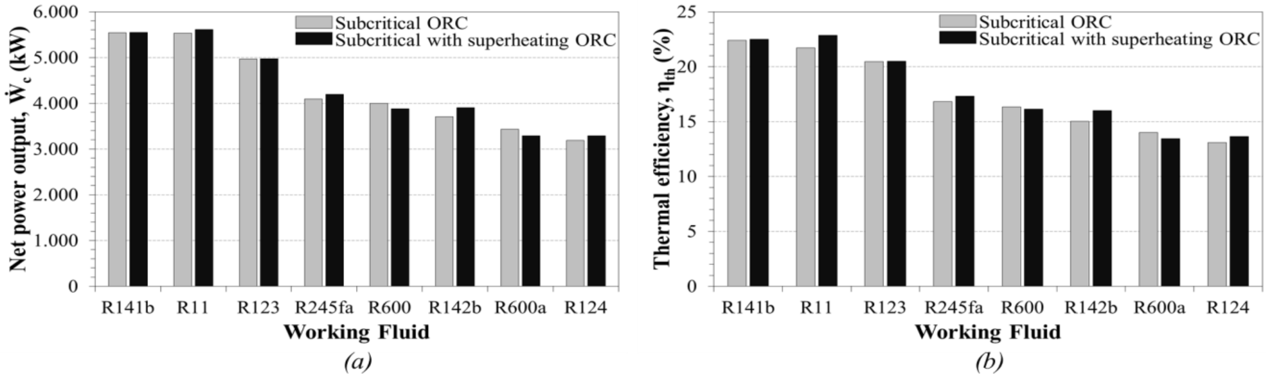

Fig. 4. Comparison of the subcritical and subcritical with superheating operating conditions results: a) net power output, b) thermal efficiency.

As expected from the thermodynamic point of view, the performance of a cogeneration system with superheating was superior to a cycle without this resource due to its greater average temperature of heat addition. Therefore, the operating condition, known as subcritical with superheating, offers favorable overall effectiveness for the ORC.

3.2. Economical results with optimization of $\dot{W}_c$

By virtue of the large volume of results acquired in the previous analysis, the economical approach focused on the three working fluids, which accomplished the best system efficiencies during the thermodynamic modeling. Only the isentropic fluids R141b, R11 and the dry fluid were considered in this stage.

According to the results, the isentropic fluid R141b reached the less expensive total capital cost for both operating conditions as shown in Fig. 5a. Moreover, a relevant fact to be highlighted is that, although the subcritical with superheating cycle includes an additional component in comparison with the subcritical ORC, which is the superheater, the subcritical with superheating condition experienced a decline in the system total capital cost for the three organic working fluids examined. This contraction corresponded to, in average, 3.27% contrasted to the subcritical results and it is explained by the reduction in the surface area for heat transfer of the heat exchangers caused by the utilization of superheater in this operating condition as indicated in Fig. 5b. In other words, regardless of the subcritical with superheating condition contains one more equipment than the subcritical one, which hypothetically should elevate the system total capital cost, what occurred was the opposite: this extra component enabled to decrease the other heat exchangers dimensions. Thus, the subcritical with superheating condition generated a positive impact on the ORC costs.

When the object of analysis was the specific investment cost, the pattern of results seen in Fig. 5a was maintained, for this indicator is associated with both total capital cost and power produced by the cycles. Again, it was possible to generate more net power output consuming fewer financial resources with the isentropic fluid R141b. Additionally, an average decrement of 3.46% in the specific investment cost results was verified when the system operated under the subcritical with superheating condition compared to the subcritical ORC as exhibited in Fig. 5c.

From the point of view of specific electricity generation cost, the results of this parameter agreed with the other results demonstrated earlier. The working fluid with the lowest cost to produce electricity among the investigated organic fluids was the isentropic fluid R141b in the subcritical with superheating cycle. Furthermore, as represented in Fig. 5d, it was observed an average decline in the cost to generate electric energy of 1.31% in the subcritical condition with superheating in contrast with the subcritical condition.

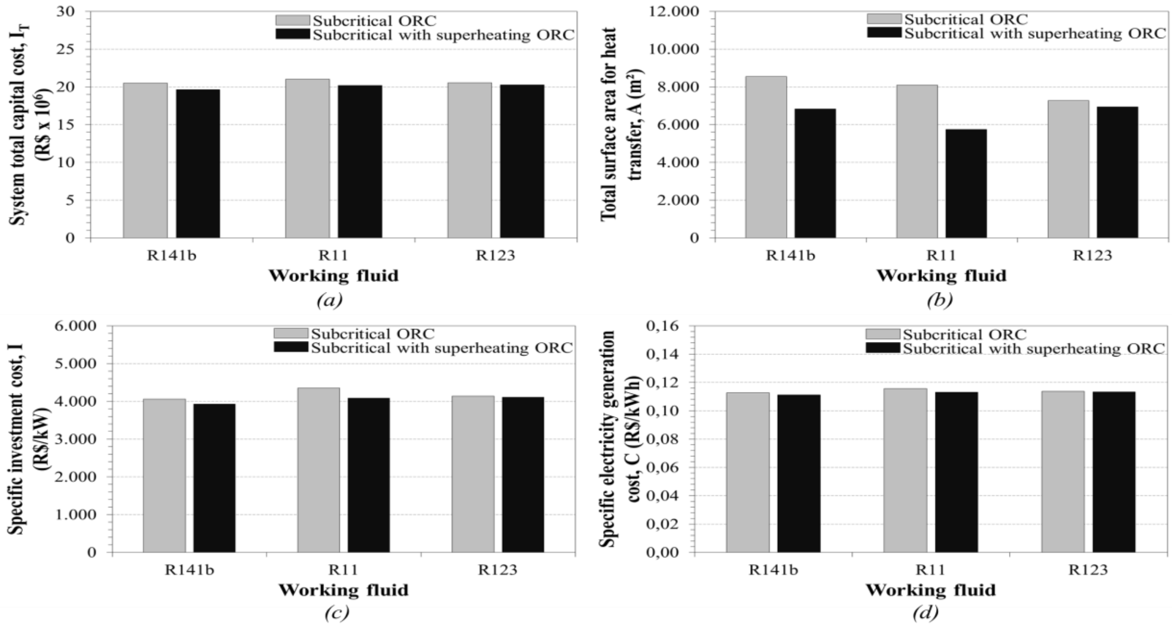

Fig. 5. Comparison of the economical modeling results: a) system total capital cost, b) total surface area for heat transfer, c) specific investment cost, d) specific electricity generation cost.

3.3. ORC results with optimization of other operating parameters

After optimizing the cycles aiming to find the highest amount of net power output produced as possible, the objective function in this step was changed so that, other operating parameters as exergy efficiency, specific investment costs and specific electricity investment costs were similarly optimized, as described in the methodology section. The results are presented and compared in Fig. 6, in which the values for the optimized net power output, second law efficiency, specific investment costs and specific electricity generation costs are illustrated by circles (●), crosses (✚), squares (■) and triangles (▲), in this order. In addition, letters (a) and (b) correspond to the subcritical and subcritical with superheating operating conditions, respectively.

Comparing the obtained results from the optimization of the net power output generated by the system, it was identified that the maximization of exergy efficiency, allowed the ORC to improve its exergy efficiency, in average, 0.21% and 2.65% for the subcritical and subcritical with superheating conditions, correspondingly. Nevertheless, this growth in the cycle's second law efficiency led to an average reduction in net power output generated of 0.72% and 3.92% in these configurations related to the results acquired when the net power output was optimized. In spite of less net power output being produced by the ORC, the growth in exergy efficiency was a result of the decrement in the amount of energy input required by the system during the working fluid evaporation process.

From the economical perspective, results revealed that when costs were minimized, the net power output generated was also reduced, for it is related to the costs composition of the cycle. The optimization of the specific investment costs produced a decrease in the net power output generated in comparison with the results acquired when the net power output was optimized, in average, of 4.34% and 0.86% for the subcritical and subcritical with superheating conditions, subsequently.

The minimization of specific electricity generation costs also induced an average contraction of net power output generated by the ORC of 3.88% for the subcritical condition and 1.54% for the subcritical with superheating operating condition. Moreover, the average declines in specific investment costs and specific electricity generation costs were, in this order, 3.31% and 1.20% for the subcritical condition, while these decrements were, respectively, 1.36% and 0.47% for the subcritical with superheating condition. Finally, the isentropic fluid R141b achieved the most competitive results among the examined organic fluids form the context of specific investment costs (3,917 R$/kW) and specific electricity generation costs (0.1112 R$/kWh).

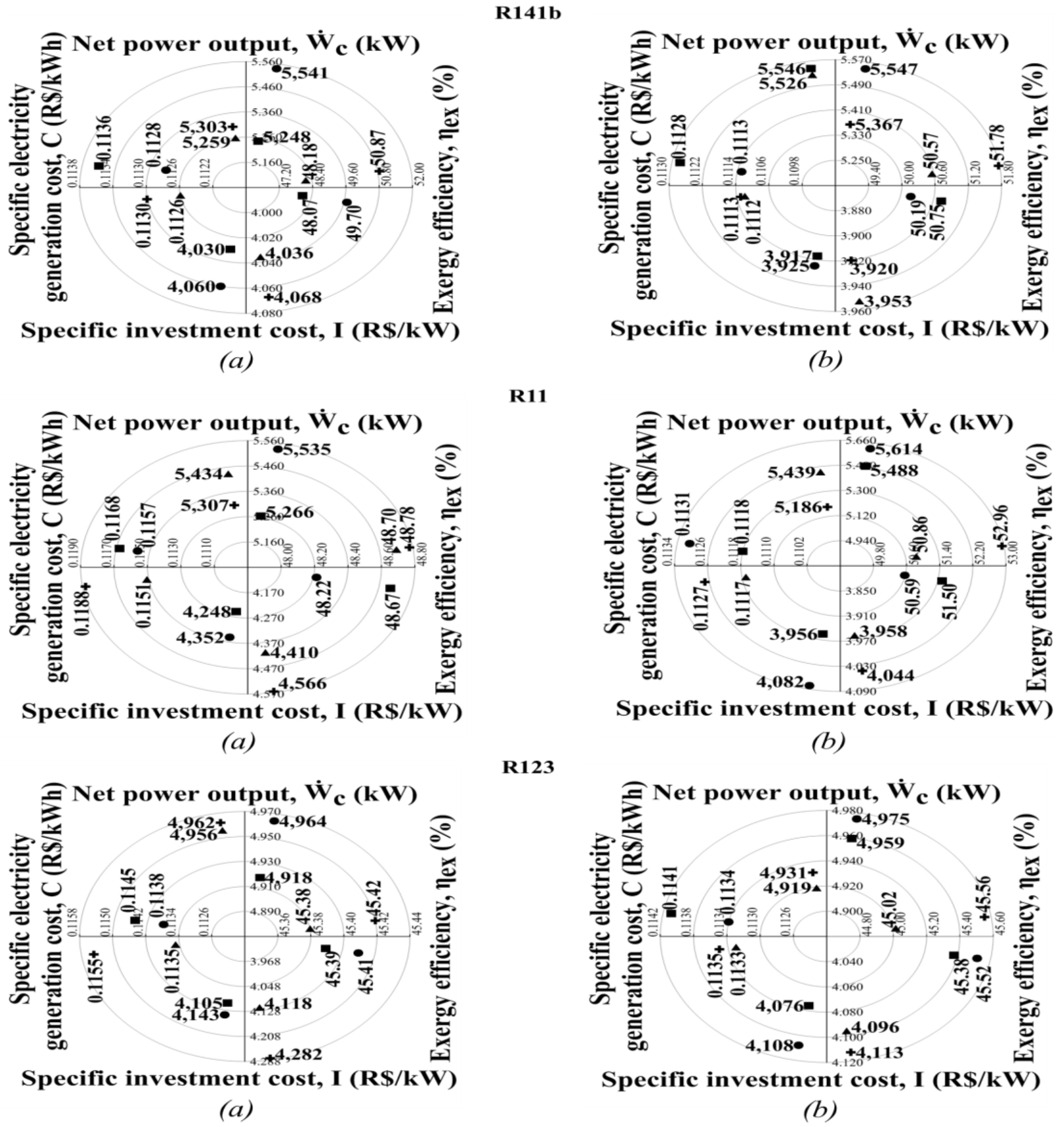

Fig. 6. Results of the other optimized operating parameters for three different working fluids.

4. Conclusions

The conclusion of the analysis of a regenerative ORC for WHR in cement process are:

- Enhancing the thermodynamic average temperature during the heat addition process in the evaporation unit is an effective approach to increase the overall ORC effectiveness.
- The subcritical with superheating condition presented superiority over the subcritical one for most of the organic working fluids analyzed in terms of net power output, thermal and exergy efficiencies, in average, 2.06%, 3.10% and 2.99%, correspondingly;
- The isentropic fluid R141b achieved best results for the subcritical condition, while other isentropic fluid, R11, performed more effectively for the subcritical with superheating condition;
- The utilization of a superheater allowed reducing the total surface area for heat transfer. Hence, it was possible to work with smaller heat exchangers and to minimize the specific investment and specific electricity generation costs, in average, 3.46% and 1.31%, subsequently;
- The isentropic fluid R141b presented superior economical results in the studied ORC.

Acknowledgments

The authors acknowledge the support provided by the Foundation for Research Support of Minas Gerais (FAPEMIG) via PPM-00381-16 project, the Pontifical Catholic University of Minas Gerais (PUC Minas) and the Coordination for the Improvement of Higher Education Personnel (CAPES).

References

[1] International Finance Corporation. Waste Heat Recovery for the Cement Sector: Market and Supplier Analysis 2014 – Available at: <http://www.ifc.org> [accessed 12.1.2017].

[2] Eyidogan M., Kilic F., Kaya D., Coban V., Cagmanc S., Investigation of Organic Rankine Cycle (ORC) technologies in Turkey from the technical and economic point of view. Renewable and Sustainable Energy Reviews 2016; 58: 885-895.

[3] Lecompte S., Huisseune H., Broek M., Paepe M., Methodical thermodynamic analysis and regression models of organic Rankine cycle architectures for waste heat recovery. Energy 2015; 87: 60-76.

[4] Li G., Organic Rankine cycle performance evaluation and thermoeconomic assessment with various applications part II: Economic assessment aspect. Renewable and Sustainable Energy Reviews 2016; 64: 490-505.

[5] Tchanche B.; Pétrissans M.; Papadakis G., Heat resources and organic Rankine cycle machines. Renewable and Sustainable Energy Reviews 2014; 39: 1185-1199.

[6] Wang X., Li X. P., Li Y. R., Wu C., Payback period estimation and parameter optimization of subcritical organic Rankine cycle system for waste heat recovery. Energy 2015; 88: 734-745.

[7] Tchanche B., Lambrinos G., Frangoudakis A., Papadakis G., Low-grade heat conversion into power using organic Rankine cycles – A review of various applications. Renewable and Sustainable Energy Reviews 2011; 15: 3963-3979.

[8] American Society of Heating, Refrigerating and Air-Conditioning Engineers, 2009 ASHRAE Handbook: Fundamentals. Inch-pound edition. Atlanta, USA: ASHRAE; 2009.

[9] Li C.; Wang H., Power cycles for waste heat recovery from medium to high temperature flue gas sources from a view of thermodynamic optimization. Applied Energy 2016; 180: 707-721.

[10] Lecompte S., Huisseune H., Broek N., Vanslambrouck B., Paepe M., Review of organic Rankine cycle (ORC) architectures for waste heat recovery. Renewable and Sustainable Energy Reviews 2015; 47: 448-461.

[11] Hung T., Waste heat recovery of organic Rankine cycle using dry fluids. Energy Conversion and Management 2001; 42: 539-553.

[12] Embraco. Informativo técnico: Isobutano (R600a) como refrigerante em sistemas herméticos de refrigeração – Available at: <http://www.embraco.com> [accessed 19.3.2017].

[13] Moreira L., Arrieta F., Barbosa Junior E., Horta G., Working fluid selection and optimization of ORC for WHR in cement production process. In: Lopez R., Miguel L., Farias P., editors. CILAMCE 2017: Proceedings of the XXXVIII Iberian Latin-American Congress on Computational Methods in Engineering; 2017 Nov 5-8; Florianópolis, Brazil.

[14] Bejan, A., Advanced engineering thermodynamics. Hoboken, USA: John Wiley & Sons; 2006.

[15] Ulrich G., Vasudevan P., Chemical engineering process design and economics: a practical guide. Durham, N. H.: Process Pub.; 2004.

[16] Companhia de Cimento Apodi. WHR system. 2015. Quixeré, Brazil. 15 slides: color.

[17] Wang J., Dai Y., Gao L., Exergy analyses and parametric optimizations for different cogeneration power plants in cement industry. Applied Energy 2009; 86(6): 941-948.

[18] Whittaker P., Corrosion in the Kalina cycle: An investigation into corrosion problems at the Kalina cycle geothermal power plant in Húsavík [dissertation]. Akureyri, Iceland: University of Iceland & The University of Akureyri; 2009.

[19] California State BOE. State of California Equipment and Fixtures Index, Percent Good and Valuation Factors – Available at: <https://www.boe.ca.gov/ > [accessed 6.8.2017].

[20] Elson A., Tidball R., Hampson A., Waste Heat to Power Market Assessment – Available at:< https://info.ornl.gov/> [accessed 10.8.2017].